

Some Formal Aspects of Tedmon's Kinetics: Growth and Sublimation of Ge₃N₄

Irakli NAKHUTSRISHVILI*

Abstract

The work considers the formal kinetics of growth of a scale with its simultaneous sublimation. The basis of the model is the power (parabolic, cubic) law of the mass gain of system "metal (alloy) – scale", with the input of an additional parameter – rectilinear constant of the speed of the process. The gained equations are used to describe the growth of Ge₃N₄ on the surface of monocrystalline germanium in humid ammonia with simultaneous sublimation of nitride.

Keywords: Scale Sublimation, Tedmon's Kinetic, Thermogravimetric Curves, Ge₃N₄

Introduction

In certain cases, the formation of a scale on the surface of metal or alloy is followed by its sublimation. The kinetics of this process (Tedmon's kinetics) has been investigated more than once both, in the past and recently [1-10]. The given model assumes that the absence of the secondary process of sublimation, the growth of the scale takes place by a "simple" parabolic law $m^2 = k_p t$ where m is the mass gain per unit area of the sample by the moment of time t , k_p is oxidation (chloridation, nitridation, etc.) parabolic rate constant.* The differential form of this law, i.e. the speed of mass gain is as follows:

$$(1) \quad \frac{dm}{dt} = \frac{k_p}{2m}$$

In case of the scale sublimation, the constant of the relevant speed (k_s) is subtracted from the right-hand side of Eq. (1):

$$(2) \quad \frac{dm}{dt} = \frac{k_p}{2m} - k_s$$

Works [8, 11] consider the growth of a scale with simultaneous sublimation, based on cubic law $m^3 = k_c t$, where k_c is cubic constant of the process speed. In this case:

$$(3) \quad \frac{dm}{dt} = \frac{k_c}{3m^2} - k_s$$

From Eqs.(2) and (3), we gain that $dm/dt \rightarrow 0$ when $m \rightarrow k_p/2k_s$ and, $m \rightarrow \sqrt{k_c/3k_s}$, respectively, i.e. power-law dependence $m(t)$ in case of sublimation of a scale is transformed into the asymptotic dependence. Besides, according to the equations above, when $t=0, m=0 \Rightarrow dm/dt = \infty$ Infinity of the initial instant speed of process may be eliminated by using the equation of "complex" parabola developed by U.R. Ewans [12] (in case of parabolic kinetics). Formally, it can be presented as $(m^2/k_p) + (m/k_r) = t$, where $k_r \equiv (\frac{dm}{dt})_{t=0, m=0}$ is a rectilinear constant of the speed of mass gain. In

such a case, with the scale sublimation, instead of Eq. (2), we will gain the following equation:

$$(4) \quad \frac{dm}{dt} = \frac{k_p/2}{m + k_p/2k_r} - k_s$$

Such a model can be used for the processes, characterized by not high values of constant k_r [13,14]**. The present report considers the question of using a similar approach for the cubic law of mass gain. On the example of nitridation of monocrystalline germanium in humid ammonia, the possibility of using the gained equations in processing the experimental data is demonstrated.

In the equations above m is the overweight of system "metal (alloy) – scale" at the expense of active gas, used (consumed) to produce the reaction product. In the absence of scale sublimation, m determines the total mass change of system (M): $M=m$. In case of scale sublimation, $M=m-m_p$, where m_p is the mass of sublimed part of the scale. It may be presented as the sum of masses of the metallic (m_m) and gaseous (m_g) components: $m_p = m_m + m_g$. Consequently, for sublimation speed (v), the following is true: $v_p = v_m + v_g$. The speed of total mass change of the system is a follows:

$$(5) \quad \frac{dM}{dt} = \frac{k_n/n}{m^{n-1} + k_n/nk_r} - v_p = \frac{k_n/n}{m^{n-1} + k_n/nk_r} - v_g - v_m$$

where in case of a parabolic process, $n=2, k_n = k_p, v_g = k_s$ and in case of a cubic process, $n=3, k_n = k_c, v_g = k_s$. The speed of the system mass change at the expense of active gas according to Eq.(5) is:

* The process is considered from the view of parabolic increase of the thickness or the mass of a scale in time. The experiment in the present work, like in the majority of the cited works, was accomplished by the thermogravimetric method. Therefore, it is preferable to use the formulas of mass changes.

** These works consider Tedmon's kinetics based on "complete" parabolic equation $(m^2/k_p) + (m/k_r) = t + t_0$. Here t_0 is the shift along the time axis, corresponding to the presence of certain value $m = m_0$ when $t=0$. Such a model is used when some process must be considered not from the zero moment of time [15].

* Ph.D, Senior Researcher of Institute of Cybernetics, Georgian Technical University, Tbilisi, Georgia.
 E-mail: gvipgirl@gmail.com

$$(6) \quad \frac{dm}{dt} = \frac{k_n / n}{m^{n-1} + k_n / nk_r} - v_g$$

As it is seen from Eq. (6), value $m_{\max} \equiv m_{dm/dt \rightarrow 0} = \left(\frac{(k_r - v_g) k_n}{nk_r v_g} \right)^{\frac{1}{n-1}}$ is the maximum overweight of the system occurring at the expense of active gas. From Eq.(6), it is also clear that instant speed of increase m at the origin of coordinates is difference $k_0 \equiv \left(\frac{dm}{dt} \right)_{t=0, m=0} = k_r - v_g$. By using these denotations, we will gain the following implicit dependence in the general case:

$$(7) \quad t = \left(1 + \frac{v_g}{k_0}\right) \left(\frac{m_{\max}^{n-1}}{v_g}\right) \int \frac{dm}{m_{\max}^{n-1} - m^{n-1}} - \frac{m}{v_g}$$

For n=2 and 3, with initial condition t=0, m=0, consequently, we will gain the following expression:

$$(8) \quad t = -(1+k) \frac{m_{\max}}{v_g} \ln \frac{m_{\max} + m}{m_{\max} - m} - \frac{m}{v_g}$$

$$(9) \quad t = (1+k) \frac{m_{\max}}{2v_g} \ln \frac{m_{\max} + m}{m_{\max} - m} - \frac{m}{v_g}$$

where $k = v_g / k_0$

When $k_r, k_0 \rightarrow \infty (i.e. k = 0)$, Eqs. (8) and (9) are transformed into the equations, which, through various modifications (not only from the view of formal kinetics, but also by considering the mechanism of the process) are given in the above-cited works.

As for the total mass change of system "metal(alloy)-scale", it can be represented only in a parametric form:

$$(10) \quad M = pm + q \left(1 + \frac{v_g}{k_0}\right) m_{\max}^{n-1} \int \frac{dm}{m^{n-1} - m_{\max}^{n-1}}$$

where $q = v_m / v_g, p = q + 1 = v_p / v_g$

and as for parameter it serves $m = M + v_m t$

Figure 1 schematically shows the typical kinetic dependences of the process in question. As m increases asymptotically, the change of M is more complex: its primary growth is gradually suppressed and is transformed into the rectilinear reduction of mass. The inclination of this line corresponds to value v_m . The described course of dependence M(t) suggests the presence of point of maximum. Such (containing maximums) kinetic curves of the total mass change are gained experimentally in a number of works cited above, as well as many other works dedicated to both, isothermal [16-18] and cyclic [19-22] processes.

From Eq.(5), it follows that the curve of total mass change has its maximum in case of the following value of parameter m:

$$\bar{m} \equiv m_{dm/dt \rightarrow 0} = \left(\frac{(k_r - v_g) k_n}{nv_p k_r} \right)^{\frac{1}{n-1}} = m_{\max} \frac{v_g}{v_p} \left(1 - \frac{v_m}{k_0}\right)$$

The coordinates of point of maximum are:

$$(11) \quad \bar{t} = \frac{m_{\max}}{v_g} \{f(1 - qk) - (1 + k) \ln[1 - f(1 - qk)]\}$$

$$(12) \quad \bar{M} = m_{\max} \{(1 - qk) + q(1 + k) \ln[1 - f(1 - qk)]\}$$

where $f \equiv 1/p$

The condition for presence of such a maximum is as follows:

$0 \leq qk < 1 \Rightarrow \frac{k_n}{v_m} > 1$ i.e. dominance of instant speed of mass gain at the expense of active gas at the origin of coordinates over the rate of the system mass reduction at the expense of the metallic component of the sublimed part of a scale. By determining values $\bar{t}, \bar{M}, v_m, k_0$ (or $K_0 \equiv \left(\frac{dM}{dt}\right)_{t=0, M=0} = K_0 - v_m$) and m_{\max} through the experimental thermogravimetric curve of a concrete process, the constants of the rate of the process can be calculated:

$$(13) \quad k_r = k_0 + v_g = k_0 + \frac{v_m}{q} = K_0 + v_p = K_0 + \frac{p}{q} v_m$$

$$(14) \quad k_n = (1 + k) n v_m m_{\max}^{n-1} / q = (1 + k) n v_p \bar{m}^{n-1}$$

where $\bar{m} = \bar{M} + v_p \bar{t}$

The Eqs. (8) and (9) show that the change of parameter $k = v_g / k_0$ changes the slopes of the kinetic dependences and obviously influences this slope of value n. Figure 2 graphically shows Eq.(7) in normalized coordinates for different values of n and k. As the Figure shows, the identification of the membership of a concrete experimental dependence to some or other power law may be complicated. In this connection, it will be useful to identify value n with the same parameters what can be easily done by comparing Eqs.(5), (11-14):

$$(15) \quad n = \frac{\lg[f(1 - qk)\bar{y}]}{\lg \bar{y}}$$

where $\bar{y} \equiv \bar{m} / m_{\max} = (\bar{M} / m_{\max}) + (v_g \bar{t} / m_{\max})$

At $k_0, K_0 \rightarrow \infty$ Eq.(15) simplified as

$$(16) \quad n = \frac{\lg(f\bar{y})}{\lg \bar{y}}$$

The formulas above can be used to analyze the literary data; for instance, let us consider work [2]. This work explores chloridation of lead at 300° by a thermogravimetric method. The production of the reaction product (PbCl₂) was accompanied by its sublimation. The author describes the process by using the model with the combination of "paralinear" [23] and Tedmon's kinetics. For approximately 160 hours of reaction, a kinetic curve for the total mass change with a clearly expressed maximum ($\bar{t} \cong 59h, \bar{M} \cong 0.72mg/cm^2$) is gained. By inserting the values of these and other typical parameters in Eq.(14), the value of constant of the speed of process (parabolic mechanism of chloridation) close to the one calculated in the original work is gained. As for Eq. (16), it is used to gain $n \cong 1.70$ what is also close to n=2.

The present work includes experiments of nitridation of monocrystalline germanium with ammonia with various degree of humidity. This reaction is of interest if considering the prospective uses of its product (Ge₃N₄) in electronics, photocatalysis and other technological areas [24, 25]. Ge(111) plates doped with stibium (concentration of the charge carrier of $2 \cdot 10^{14} cm^{-3}$, specific resistance of $35 \pm 0.5 \Omega \cdot cm$). The samples of germanium were treated in etchant HF: HNO₃: CH₃COOH = 1:15:1. The used ammonia contained 99.6% NH₃ and (0.2-0.4)% H₂O. Experiments were accomplished in static vacuum conditions by means of continuous weighing of the sample with the microbalance with automated electro-magnetic compensation of weight changes (sensitivity of 10⁻⁶g). The temperature of the process was 800-820°C.

Figure 3 shows the thermogravimetric curves of nitridation of germanium. Their general view – passing through the point of maximum with a rectilinear decrease of the sample mass at the final stage – indicates the sublimation of produced nitride. This is also

evidenced by the precipitation of an amorphous film in the "cold" (300–350°C) area of the reactor. According to Auger-spectroscopic analysis, this film is a germanium oxynitride. The presence of oxygen in the film is due to the presence of water vapor in the reaction area [26].

Curve 1 in Figure 3 is obtained during the interaction of germanium with ammonia at temperature 820°C. Nitride formed on the surface of Ge was the β-modification of Ge₃N₄ *. The panel of Fig. 3 shows the initial branch of curve 1. The values of the typical parameters are: $\bar{t} \cong 4.5 \text{ min}$, $\bar{M} \cong 1.2 \cdot 10^{-2} \text{ mg/cm}^2$, $k_0 \cong 2 \cdot 10^{-2} \text{ mg/cm}^2 \text{ min}$, $v_m \cong 9.6 \cdot 10^{-3} \text{ mg/cm}^2 \text{ min}$, $m_{max} \cong 1.45 \cdot 10^{-1} \text{ mg/cm}^2$. By considering these values and that $q = M_{3Ge}/M_{4N} \cong 3.89$ and $p = M_{Ge3/4}/M_{4N} = q + 1 \cong 4.89$ Eq. (15) can be used to gain $n \cong 3.32$. The proximity of this value to 3 allows using Eq.(9). Its empiric form will be: $t \cong 0.550/n[(0.145 + m)/(0.145 - m)] - 6.753m$ where m is given in terms of mg/cm^2 and t is measured with hours. As for formulas (13) and (14), the following values are gained: $k_r \cong 4.47 \cdot 10^{-3} \text{ g/m}^2 \text{ sec}$ and $k_s \cong 2.68 \cdot 10^{-3} \text{ g}^3/\text{m}^2 \text{ sec}$. Curve 2 in Figure 3 is obtained for specially adding the water vapor to the reaction area (95.2% NH₃, (4.7–4.8)% H₂O). In this case, at 800°C on the surface of germanium, a mixture of α- and β-modifications of Ge₃N₄ with dominating content of β-phase was produced. The typical parameters of the curve in question are: $\bar{t} \cong 7.5 \text{ min}$, $\bar{M} \cong 2 \cdot 10^{-2} \text{ mg/cm}^2$, $k_0 \cong 6 \cdot 10^{-2} \text{ mg/cm}^2 \text{ min}$, $v_m \cong 2.62 \cdot 10^{-2} \text{ mg/cm}^2 \text{ min}$, $m_{max} \cong 1.42 \text{ mg/cm}^2$. In compliance with these values, Eqs. (15), (13) and (14) give the following values: $n \cong 2.15$, $k_r \cong 1.11 \cdot 10^{-2} \text{ g/m}^2 \text{ sec}$, $k_s \cong 3.55 \cdot 10^{-2} \text{ g}^2/\text{m}^2 \text{ sec}$. The empirical form of Eq. (8) will be: $t \cong -3.908 \ln(1 - 0.704m) - 2.475m$ where m is given in terms of mg/cm^2 , and t is measured with hours.

In addition to the experimental curves (with variance M), Figure 3 shows the curves of increase of m (1,2) and curves ($\bar{1}, \bar{2}$) according to the empirical expressions given above. Curve $\bar{1}$ gets satisfactorily closer to curve $\bar{1}$. The correspondence between the curves 2 and ($\bar{2}$) is less satisfactory. However, as P.Kofstad [29] noted, all kinetic equations of the scale growth show only ideal or limit cases: compliance of the calculated and experimental data with a certain approximation can be considered acceptable. The dotted curves in the same figure show the rated dependences gained from the assumption in Eqs. (8) and (9) when $k = 0(k_r, k_0 \rightarrow \infty)$. The discrepancy between them and the experimental curves is even greater.

Thus, the considered model can be used to describe the process of growth of a nitride layer on the surface of germanium with its simultaneous sublimation. Presumably, it can also be used for other Tedmon's processes by considering the real values of initial instantaneous speed of the process.

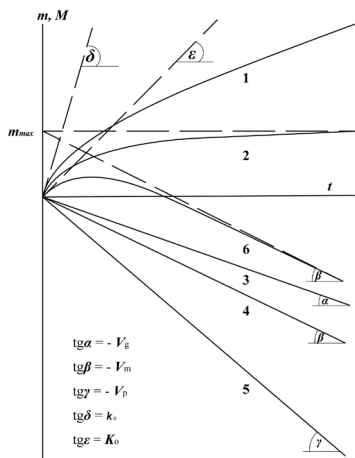


Figure 1. Graphs of kinetic dependences of: the metal overweight at the expense of active gas, in the absence (1) and presence (2) of scale sublimation; the reduction of the system mass due to the gaseous (3) and metallic component (4) of the sublimated product, and product itself (5); the total change of the mass of system(6).

References

- Tedmon, C.S. (1966). The Effect of Oxide Volatilization on the Oxidation Kinetics of Cr and Fe-Cr Alloys. *Electrochemical Society*, 113(8), 766-768.
- Weijzel, D. (1963). A Method for Calculating Parabolic Constants for the Formation of Volatile Scale. *Electrochemical Society*, 110(6),
- Haanappel, V.A., Fransen, T., Gellings, P.J. (1992). Chlorine Induced High-Temperature Corrosion: the Tedmon Equation as a Theoretical Approach of the Kinetics. *High Temperature Materials and Processes*, 10(2), 91-100..
- Opila, E.J. (2003). Oxidation and Volatilization of Silica Formers in Water Vapor. *American Ceramic Society*, 86(8), 1238-1248.
- Nickel, K.G. (2005). Ceramic Matrix Composite Corrosion Models. *European Ceramic Society*, 25(10), 1699-1704.
- Berthod, P. (2005). Kinetics of High-Temperature Oxidation and Chromia Volatilization for a Binary Ni-Cr Alloy. *Oxidation of Metals*, 64, (3/4), 235-252.
- Pujilaksono, B., Jonsson, T., Halvarsson, M., Panas, I., Svensson, J.-E., Johansson, L.-G. (2008). Parabolic Oxidation of Chromium in O₂+H₂O Environment at 600-700C. *Oxidation of Metals*, 70(3/4), 163-188.
- Chen, Y., Tan, T., Chen, H. (2008). Oxidation Companioned by Scale Removal: Initial and Asymptotic Kinetics. *Nuclear Science and Technology*, 45(7), 662-667.
- Latreche, H. (2009). Development of Protective Coatings to Improve High-Temperature Corrosion Resistance in Chlorine Containing Environments Based on an Advanced Corrosion Risk Assessment Tool. *Frankfurt*, 156.
- Zhu, S., Feng, Z., Liu, J. (2014). Kinetics Modeling of Parabolic Growth Competing to Linear Declining: a Theoretical Tool to Interpret Corrosion Data in Real World. *Advanced Materials Research*, 860-863, 899-902.
- Nakhutsrishvili, I.G. (2006). Growth of Scale According to the Third Order Power Law with Simultaneous Sublimation. *Proceedings of the Georgian Academy of Sciences, Chemical Series*, 32(3/4), 445-447.
- Evans, U.R. (1960). *The Corrosion and Oxidation of Metals: Scientific Principles and Practical Applications*. London, Arnold LTD, 272.
- Prantsevich, I.N., Voytovich, R.F, Lavrenko, V.A. (1963). *High-Temperature Oxidation of Metals and Alloys*. Kiev, Publishing House of Technical Literature of Ukrainian SSR, 322.
- Nakhutsrishvili, I.G. (2005). Kinetic Description of the Scale Growth Based on the General Parabolic Equation, *Ferrous Metallurgy*, 5, 36-39.
- Pieraggi, B. (1987). Calculations of Parabolic Reaction Rate Constants. *Oxidation of Metals*, 27(3/4), 177-185.
- Jones, E.S., Mosher, J.F., Speiser, R., Spretnak, J.W. (1958). The Oxidation of Molybdenum. *Corrosion*, 14(1), 20-26.
- Hassel, A.W., Neelakantan, L., Zelenkevych, A., Ruh, A., Spiegel, M.(2008). Selective de-Alloying of NiTi by Oxochloridation. *Corrosion Science*, 45(7), 662-667.

* Among the crystalline modifications Ge₃N₄ only the phases with the structure of a phenacite-type (α & β) are stable at common temperatures and pressures [27]. The difference between α- and β-modifications lies in the joint of tetrahedrons Ge(N₄) in the direction of axis C in a hexagonal unit cell [28].

Falk-Windisch, H., Svensson, J.E., Froitzheim, J. (2015). The Effect of Temperature on Chromium Vaporization and Oxide Scale Growth on Interconnect for Solid Oxide Fuel Cells. *Power Sources*, 287, 25-35.

Smialek, J.L., Auping, J.V. (2002). COSP for Windows-Strategies for Rapid Analyses of Cyclic-Oxidation Behavior. *Oxidation of Metals*, 57(5/6), 559-581.

Pint, B.A., Tortorelli, P.F., Wright, I.G. (2002). Effect of Cycle Frequency on High-Temperature Oxidation Behavior of Alumina-Forming alloys. *Oxidation of Metals*, 58,(1/2), 73-101.

Sureau, S., Poquillon, D., Monceau, D. (2007). Numerical Simulation of Cyclic Oxidation Kinetics with Automatic Fitting of Experimental Data. *Scripta Materialia*, 56(3), 233-236.

Chatterjee, A., Srikanth, S., Sanyal, S., Krishna, L., Anand, K., Subramanian, P.R. (2011). Kinetic Modeling of High-Temperature Oxidation of Ni-base Alloys. *Computational Materials Science*, 50, 811-819.

Haycock, E.W. (1959). Transitions from Parabolic to Linear Kinetics in Scaling of Metals. *Electrochemical Society*, 106(9), 771-775.

SiGe, Ge, and Related Compounds 4, Eds.: Haramé, D., Boquet, J. et al. (2010). *ECS Transactions*, 33(6), 1034.

Photoelectrochemical Water Splitting, Eds.: Lewerenz, H.-J., Peter, L. (2013). *RSC Energy and Environment Series*, 9, 467.

Aronishidze, M.N., Nakhutsrishvili, I.G., Wardosanidze, Z.V.(2015). The Gas Etching of a Monocrystalline Germanium Surface. *Proceedings of the Georgian Academy of Sciences, Chemical Series*, 41(4), 361-365.

Cang, Y., Yao, X., Chen, D., Yang, F., Yang, H. (2016). First-Principles Study on the Electronic, Elastic and Thermodynamic Properties of Three Novel Germanium Nitrides. *Semiconductors*, 37(7), 072002(1-7).

Ruddlesden, S.N., Popper, P. (1958). On the Crystal Structures of the Nitrides of Silicon and Germanium. *Acta Crystallographica*, 11, 7, 465-469.

Kofstad, P. (1966). *High-Temperature Oxidation of Metals*. New York-London-Sydney, J.Wiley&Sons, 340.

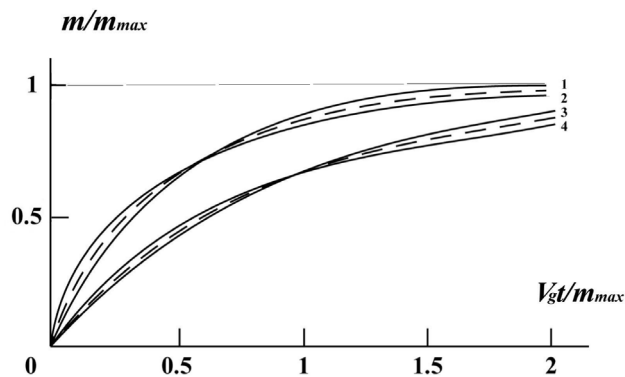


Figure 2. Curves drawn according to Equation (7) for: $n=3, k=0.3$ (1); $n=2, k=0$ (2); $n=3, k=1$ (3) and $n=2, k=0.5$ (4) in normalized coordinates. Dotted lines are the hypothetical curves of the system mass increase at the expense of active gas. (1) and (3) are given according to Eq.(9), (2) and (4) - to Eq.(8).

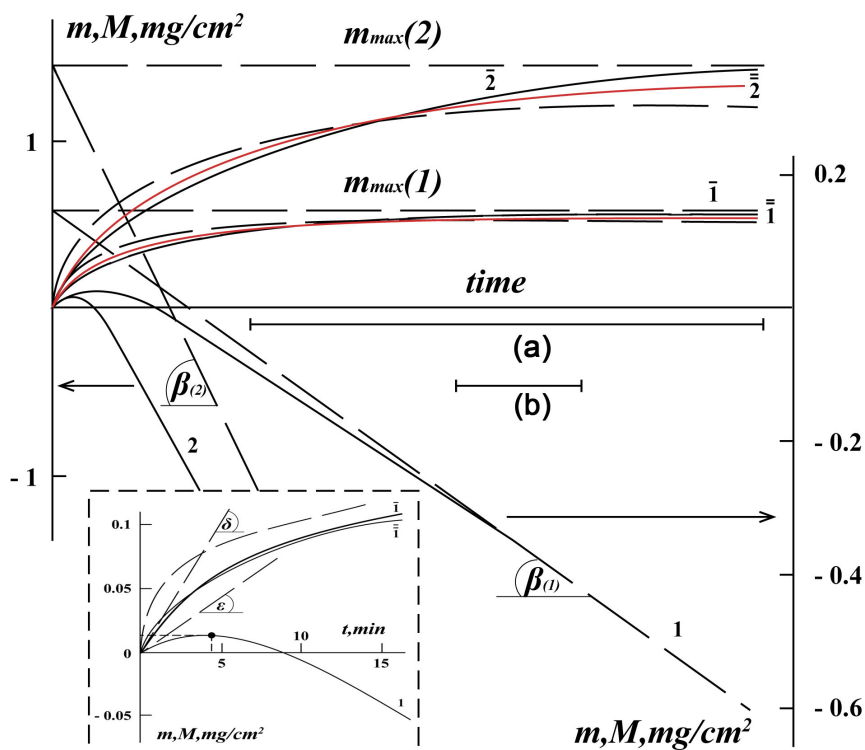


Figure 3. Thermogravimetric curves of interaction of germanium with humid ammonia: in case of production of $\beta\text{-Ge}_3\text{N}_4$ (1,1) and in case of $\alpha, \beta\text{-Ge}_3\text{N}_4$ (2,2). 1 and 2 are corresponding calculated curves; the scale of time axis (1 hour): for curves 1, 1-bar (a) and for curves 2, 2-bar (b). The panel gives the initial branches of curves 1, 1-bar. (The notations of angles correspond to Figure 1.)